Journal of Experimental Botany, Vol. 69, No. 18 pp. 4443–4457, 2018
doi:10.1093/jxb/ery227 Advance Access publication 20 June 2018

RESEARCH PAPER

The calcium sensor TaCBL4 and its interacting protein TaCIPK5 are required for wheat resistance to stripe rust fungus

Peng Liu†, Yinghui Duan†, Cong Liu, Qinghe Xue, Jia Guo, Tuo Qi, Zhensheng Kang* and Jun Guo*

State Key Laboratory of Crop Stress Biology for Arid Areas, College of Plant Protection, Northwest A&F University, Yangling, Shaanxi 712100, P. R. China

* Correspondence: guojunwgq@nwsuaf.edu.cn or kangzs@nwsuaf.edu.cn

† These authors contributed equally to this work.

Received 9 November 2017; Editorial decision 6 June 2018; Accepted 8 June 2018

Editor: Steven Spoel, University of Edinburgh, UK

Abstract

Calcineurin B-like proteins (CBLs) act as Ca^{2+} sensors to activate specific protein kinases, namely CBL-interacting protein kinases (CIPKs). Recent research has demonstrated that the CBL–CIPK complex is not only required for abiotic stress signaling, but is also probably involved in biotic stress perception. However, the role of this complex in immune signaling, including pathogen perception, is unknown. In this study, we isolated one signaling component of the TaCBL–TaCIPK complex (TaCBL4–TaCIPK5) and characterized its role in the interaction between wheat (*Triticum aestivum*) and *Puccinia striiformis* f. sp. *tritici* (*Pst*, stripe rust fungus). Among all *TaCBL*s in wheat, *TaCBL4* mRNA accumulation markedly increased after infection by *Pst*. Silencing of *TaCBL4* resulted in enhanced susceptibility to avirulent *Pst* infection. In addition, screening determined that TaCIPK5 physically interacted with TaCBL4 *in planta* and positively contributed to wheat resistance to *Pst*. Moreover, the disease resistance phenotype of *TaCBL4* and *TaCIPK5* co-silenced plants was consistent with that of single-knockdown plants. The accumulation of reactive oxygen species (ROS) was significantly altered in all silenced plants during *Pst* infection. Together these findings demonstrate that the TaCBL4–TaCIPK5 complex positively modulates wheat resistance in a ROS-dependent manner, and provide new insights into the roles of CBL–CIPK in wheat.

Keywords: Calcineurin B-like protein (CBL), CBL-interacting protein kinases (CIPK), disease resistance, reactive oxygen species, wheat stripe rust.

Introduction

Plants respond to the perception of external stimuli, including abiotic and biotic stresses, through a rapid activation of numerous signaling pathways, thereby enabling them to defend against impending stress (Pandey, 2008). The concentration of intracellular Ca^{2+} in cells undergoes transient changes in response to these stimuli and functions as a second messenger to regulate a plethora of inter- and extracellular signaling processes. These processes require the function of highly regulated sensors and relay proteins, such as calmodulins (CaMs), calmodulin-like proteins (CMLs), and calcineurin B-like proteins (CBLs). In each of these relay cascades, it is hypothesized that signaling is activated via a calcium-induced conformational change that is relayed to an interacting

partner, which in turn leads to a further conformational change resulting in a concomitant change in enzyme activity. In contrast, sensor responders, such as the calcium-dependent protein kinases (CDPKs), undergo a calcium-induced conformational change that alters the protein's own activity or structure. These two different modes of decoding calcium signals are used extensively in plants to provide many pathways by which calcium can trigger a diverse number of responses (Sanders *et al.*, 2002).

As another type of signaling molecule of secondary signaling processes, reactive oxygen species (ROS) have been well studied for their role in plant development and responses to environmental stimuli (Gupta *et al.*, 2015). In individual cells, the production and scavenging of ROS can be rapidly regulated, allowing dynamic control of ROS concentrations and accumulation, which results in an efficient intracellular control. Moreover, as signal transduction molecules, the ROS-induced signaling can be transmitted from the origin of the stimulus to nearby cells (Mittler *et al.*, 2011). In addition to its function as a signal molecule, the increased communication of ROS leads to programmed cell death (PCD) by impairing metabolism and damaging organelles in plant cells under abiotic and biotic stress (Zurbriggen *et al.*, 2010). Ca^{2+} has been reported to enhance cellular ROS accumulation and, vice versa, ROS can activate Ca^{2+} release (Steinhorst and Kudla, 2013).

CBLs are among a number of Ca^{2+} sensors in plant cells. They transmit signals by interacting specifically with a NAF/FISL motif in the C-terminal regulatory domain of CBL-interacting protein kinases (CIPKs), which belong to the Snf1-RELATED KINASE3 family (Suc nonfermenting 1-related kinases, group 3; SnRK3). Diverse members of the CBL and CIPK families are found exclusively in the plant kingdom (Pandey *et al.*, 2014) and, to date, bioinformatic analyses have identified 10 CBLs and 26 CIPKs in Arabidopsis (Hashimoto *et al.*, 2012), and 10 CBLs and 33 CIPKs in rice (Kanwar *et al.*, 2014). A broad range of proteins have been confirmed as targets of CIPKs, such as phosphatases, transporters/channels, transcription factors, and enzymes, indicating that the CBL–CIPK complex performs multiple and extensive roles in biological processes (Pandey *et al.*, 2014). In addition, further evidence has suggested that phosphorylation of CBL proteins by their interacting CIPKs is required for full activity of CBL–CIPK complexes (Hashimoto *et al.*, 2012).

The CBL–CIPK components have been extensively studied in relation to the regulation of different abiotic stress-triggered signaling pathways (Luan, 2009; Pandey *et al.*, 2014). In rice, overexpression of *OsCBL8* and *OsCIPK15* results in enhanced salt tolerance (Xiang *et al.*, 2007), whereas in transgenic tobacco plants, overexpression of *TaCIPK2* from wheat confers drought tolerance (Wang *et al.*, 2016). In addition, the mechanism by which the CBL–CIPK components respond to abiotic stress has been widely studied as a signaling node. For example, SOS1, a Na^+/H^+ antiporter, is phosphorylated and activated at the plasma membrane by SOS3/CBL4 and its interacting kinase SOS2/CIPK24 (Ishitani *et al.*, 2000). Under salt stress, CBL–CIPK complexes maintain ion homeostasis and provide salt tolerance through transducing a Ca^{2+} signal (Xu *et al.*, 2013). A voltage-gated inward K^+ channel (AKT1) is regulated by AtCIPK23, which results in increased K^+ uptake under low potassium conditions (Drerup *et al.*, 2013).

Compared to abiotic stress signaling, the involvement of the CBL–CIPK system in response to biotic stresses is still an understudied area of research. A few studies have indicated that certain CBLs or CIPKs may function in plant defense signaling in response to microbial infection (Pandey *et al.*, 2014). For example, in rice, OsCIPK14 and OsCIPK15 are induced by stimulation of microbe-associated molecular patterns (MAMPs), whereby suppression of OsCIPK14/15 results in a reduction of MAMP-induced ROS production (Kurusu *et al.*, 2010). In another study, NPR1, the key salicylic acid-signaling activator, was shown to be activated and phosphorylated by CIPK11, leading to induction of WRKY38 and WRKY62 within 4–12 h after bacterial inoculation (Xie *et al.*, 2010). Moreover, ROS was significantly induced by overexpressing tomato *CIPK6* in *Nicotiana benthamiana*, which required RBOHB, a protein related to ROS generation (de la Torre *et al.*, 2013). Silencing the CIPK6–CBL10 complex suppressed Pto/AvrPto-elicited PCD in tomato (Abramovitch and Martin, 2005; de la Torre *et al.*, 2013). Additionally, TaCIPK29 was also found to be involved in ROS homeostasis in wheat (Deng *et al.*, 2013), whereas CIPK6 in Arabidopsis negatively regulates effector-triggered and pathogen-associated molecular pattern (PAMP)-triggered immunity (Sardar *et al.*, 2017).

Wheat stripe rust, caused by the obligate biotrophic fungus *Puccinia striiformis* f. sp. *tritici* (*Pst*) poses a tremendous threat to the production of wheat worldwide (Wan *et al.*, 2004). The function of CBL–CIPK components against infection by *Pst* in wheat is unknown. In this study, we found that knockdown of expression of *TaCBL4* and *TaCIPK5* decreased wheat resistance to *Pst*. In addition, ROS accumulation was significantly reduced in the silenced plants. Thus, we concluded that *TaCBL4* and its interacting partner TaCIPK5 co-regulate wheat resistance partially by regulating ROS signals. Our work provides new insights towards understanding the roles of the CBL–CIPK network in wheat in response to pathogen infection and immunity.

Materials and methods

Identification and sequence analysis of CBL *gene families in wheat*

The TAIR v10 (http://www.arabidopsis.org/) and RGAP v7 (http://rice.plantbiology.msu.edu/) databases were used to collect amino acid sequences of CBLs in Arabidopsis and rice, respectively. Whole protein sequences of wheat (*Triticum aestivum*) were downloaded from the wheat genome database at EnsemblPlants (http://plants.ensembl.org/index.html) (Clavijo *et al.*, 2017). To identify the predicted *TaCBLs* in wheat, Hidden Markov Model (HMM) profiles were built from known CBLs as queries using the HMMER software (Finn *et al.*, 2011). Local HHM-based searches and BLASTp searches were performed in the wheat genome database, with all CBL sequences of rice and Arabidopsis as queries. The Pfam software (http://pfam.xfam.org) was used to validate potential TaCBL proteins identified from the wheat genome database. Protein queries that did not contain the known conserved domains or motifs were removed. Amino acid sequences of CBLs from Arabidopsis, rice, and wheat were selected to perform multiple alignments using Clustal X 2.0 (Larkin *et al.*, 2007). A phylogenetic tree of the alignments of amino acid sequences was generated with the MEGA 6.0 software (Tamura *et al.*, 2013). Pairwise identity and similarity of proteins was calculated using MatGAT v2.02 (Campanella *et al.*, 2003). Domain analysis was performed using SMART (http://smart.embl-heidelberg.de/) and PROSITE (http://prosite.expasy.org/). Motif logos were analysed and generated by using the corresponding protein sequences in the MEME

software (http://meme-suite.org/tools/meme) with default parameters. Palmitoylation sites and myristoylation sites were predicted using CSS-Palm 3.0 (http://csspalm.biocuckoo.org/) and Myristoylator (http://web.expasy.org/myristoylator/), respectively.

Plant and fungal material, RNA extraction, qRT-PCR analysis, and gene cloning

Wheat seedlings of cultivar Suwon11 were maintained and inoculated with *Pst* race CYR23 or CYR31 following methods described previously (Kang *et al.*, 2002). Suwon 11, which carries the *YrSu* resistance gene, is resistant to the *Pst* race CYR23 (avirulent) but is highly susceptible to CYR31 (virulent) (Cao *et al.*, 2002). During the interaction between wheat and *Pst*, ROS accumulation during the early infection stage is associated with the occurrence of hypersensitive cell death. According a previous study (Wang *et al.*, 2007), a rapid increase of ROS generation at infection sites can be detected within 12 h post-inoculation (hpi). In addition, the number of necrotic host cells surrounding the infection sites increased continuously after 20 hpi. For RNA extraction, second leaves inoculated with CYR23, CYR31, or sterile distilled water (control) were harvested at 0, 6, 12, 24, 48, 72, and 120 hpi: the time points were selected on the basis of the study by Wang *et al.* (2007). All samples were immediately frozen in liquid nitrogen and stored at −80 °C. Each treatment included three independent biological replicates. Total RNA was extracted using TRIzol™ Reagent (Invitrogen) according to the manufacturer's instructions. Contaminating DNA was digested with Dnase I (Promega). First-strand cDNA was synthesized using the GoScript Reverse Transcription System (Promega) and qRT-PCR reactions were performed as described by Duan *et al.* (2013). Gene expression was quantified using a 7500 Real-Time PCR System (Applied Biosystems). The wheat translation elongation factor 1α subunit gene (*TaEF*) was used as an internal reference (Wang *et al.*, 2011). qRT-PCR data were analysed using the comparative $2^{-\Delta\Delta Ct}$ method (Livak and Schmittgen, 2001). For cloning, specific primers were designed according to the identified candidate sequences, which contained the coding sequences of *TaCBLs* and *TaCIPK5* (see Supplementary Table S2 at *JXB* online).

Sequence analysis of TaCBL4 and TaCIPK5

To confirm the copies of *TaCBL4* and *TaCIPK5* in the wheat cv. Chinese Spring genome, *TaCBL4* and *TaCIPK5* were aligned with data from the EnsemblPlants database. The predicted chromosomal location and related sequences were also obtained from this website. The cDNA sequences were analysed using ORFfinder (https://www.ncbi.nlm.nih.gov/orffinder/) and the Nucleotide BLAST and Protein BLAST programs in NCBI (https://www.ncbi.nlm.nih.gov/). The amino acid sequences were analysed with Pfam, InterProScan (http://www.ebi.ac.uk/interpro/search/sequence-search), and the ScanProsite tool (http://prosite.expasy.org/scanprosite/) to identify conserved domains. Multiple sequence alignment was performed using the DNAMAN 7.0 software (LynnonBiosoft, USA), and a phylogenetic tree of alignment of amino acid sequences was generated with the MEGA 6.0 software (Tamura *et al.*, 2013).

Deletion mutant of TaCIPK5

To make the deletion mutant (TaCIPK5Δ), the overlap-PCR approach was used. First-round PCR products were amplified with TaCIPK5-S, TaCIPK5(M)-AS, and TaCIPK5(M)-S, TaCIPK5-AS (Supplementary Table S2). The PCR products were used as templates for amplification using TaCIPK5-S and TaCIPK5-AS. The final PCR fragment was cloned into the pGEM-T Easy Vector (Promega) for sequencing. The final constructs were used as templates in yeast two-hybrid, bimolecular fluorescence complementation (BiFC), and co-immunoprecipitation (Co-IP) assays (see below).

Yeast two-hybrid assays

For interaction analyses of TaCIPK5–TaCBL4 and TaCIPK5Δ–TaCBL4, MatchMaker yeast two-hybrid assays were performed (Takara). The coding sequences of *TaCIPK5*, *TaCIPK5Δ*, and *TaCBL4* were subcloned into the pGADT7 (activation domain, AD) and pGBKT7 (DNA-binding domain, BD) vectors, respectively. The pairs of plasmids of AD and BD were then co-transformed into yeast strain AH109 by the lithium acetate method according to the Yeast Protocols Handbook (Takara). The yeast colonies were grown at 30 °C for 4 d on selection medium before they were photographed. For serial dilution, the yeast cells were collected and washed twice with sterile ultrapure water and then diluted to 10^7, 10^6, 10^5, and 10^4 cells ml^{-1}, as quantified with a hemocytometer.

Bimolecular fluorescence complementation assays

The full-length coding sequences of *TaCIPK5* and *TaCIPK5Δ* were cloned into a pUC-pSPYNE vector and fused with the N-terminal fragment of yellow fluorescent protein (YFP) to form YFP_N-*TaCIPK5* and YFP_N-*TaCIPK5Δ* constructs. The full-length coding sequence of *TaCBL4* was cloned into a pUC-pSPYCE vector as a fusion with the N-terminal fragment of YFP to form YFP_C-*TaCBL4* (Kerppola, 2008) (Supplementary Table S2). Plasmids of YFP_N-*TaCIPK5*/YFP_C-*TaCBL4* or YFP_N-*TaCIPK5Δ*/YFP_C-*TaCBL4* were then co-transformed into wheat protoplasts following the PEG-mediated transformation methods as previously described by Walter *et al.* (2004). The interaction of TaPI4KIIγ with TaUDF1 was used as the positive control (Liu *et al.*, 2013). A confocal laser scanning microscope (Leica Microsystems) was used to observe fluorescence in the protoplasts. SDS-PAGE, western blot transfer, and immunodetection using HA- and α-myc-specific antibodies (both Sungene, Tianjing, China) were performed as described previously by Walter *et al.* (2004).

Co-immunoprecipitation assays

The coding sequence of *TaCBL4* was cloned into pENTR/D-TOPO (Life Technologies, Thermo Fisher Scientific) using gene-specific DNA primers (Supplementary Table S2), then the pENTR/D-TOPO expression construct of *TaCBL4* was recombined into the pGWB11 vector using Gateway LR Clone methods (Invitrogen) to yield an N-terminal fusion to the flag-epitope. The green fluorescent protein (GFP) expression constructs *GFP-TaCIPK5* or *GFP-TaCIPK5Δ* were created by cloning the PCR-amplified ORF of *TaCIPK5* or *TaCIPK5Δ* into the *Nco*I and *Spe*I restriction enzymes sites of the binary vector pCAMBIA1302 containing an N-terminal GFP-epitope. *Agrobacterium tumefaciens* strain GV3101 carrying the gene of interest expressed from the binary vector pCAMBIA1302 and pGWB11 was grown overnight at 28 °C on LB plates containing 25 μg ml^{-1} kanamycin and 100 μg ml^{-1} rifampicin. Agro-infiltrated *N. benthamiana* leaves were collected for protein extraction, protein immunoprecipitation, and immunoblotting following methods described in a previous study (Du *et al.*, 2015).

Virus-induced gene silencing (VIGS)

Two cDNA fragments of *TaCBL4* and *TaCIPK5* (Supplementary Figs S5, S11, Table S2) with *Not*I and *Pac*I restriction sites were obtained by reverse transcription PCR and inserted into the original Barley stripe mosaic virus (BSMV) vector for gene silencing (Hein *et al.*, 2005). Fragments had no similarity to any other wheat gene in BLAST analyses (http://blast.ncbi.nlm.nih.gov/Blast/). In addition, to confirm the specificity of fragments used in the VIGS assays, the expression levels of all *TaCBLs* and several *TaCIPKs* were measured in *TaCBL4*- and *TaCIPK5*-knockdown plants, respectively. The fragment of wheat phytoene desaturase (*TaPDS*) was inserted into the BSMV vector as the positive control. The BSMV viruses (BSMV:γ, BSMV:TaPDS-as, BSMV:TaCBL4-1as/2as, and BSMV:TaCIPK5-1as/2as) were inoculated individually on wheat seedlings at the two-leaf stage following the methods described in a previous study (Hein *et al.*, 2005). The co-silencing method of *TaCBL4* and *TaCIPK5* was performed as described in a previous study (Yang *et al.*, 2013). Capped *in vitro* transcripts were prepared from linearized plasmids containing the tripartite BSMV genome using the RiboMAX TM Large-Scale RNA Production System-T7 (Promega) and the Ribo m^7G Cap Analog (Promega) according to the manufacturer's instructions. Second leaves of wheat seedlings at the two-leaf stage were infected with BSMV

constructs by rub inoculation. After incubation for 24 h in the dark in a humid environment, seedlings were placed in a growth chamber at 25 ± 2 °C. BSMV:TaPDS-1as was used as a positive control. Control plants were treated with 1× FES buffer (0.1 M glycine, 0.06 M K_2HPO_4, 1% w/v tetrasodium pyrophosphate, 1% w/v bentonite, and 1% w/v celite, pH 8.5) devoid of BSMV transcripts. The fourth leaf of each plant was then inoculated with urediospores of CYR23 or CYR31 at 10 d after inoculation with BSMV. For RNA isolation and histological observation, leaves inoculated with *Pst* were sampled at 0, 24, 48, and 120 hpi. After 15 d after inoculation with *Pst*, the infection types were examined on the basis of the McNeal measurement scale (McNeal *et al.*, 1971) and images were taken. The experiment was repeated three times. To confirm the host responses in silenced plants, the expression level of two pathogenesis-related (PR) proteins, *TaPR1* and *TaPR2*, were analysed by qRT-PCR. To confirm reduction of ROS accumulation in silenced plants, the relative transcript levels of the superoxide dismutase (*TaSOD*), catalase (*TaCAT*), and NADH-oxidase (*TaRBOHi*) genes were analysed by qRT-PCR in comparison with the control plants in each assay, as described above.

Histological observations of fungal growth and host responses

Auto-fluorescence of attacked mesophyll cells was observed as a necrotic area by epifluorescence microscopy (excitation filter, 485 nm; dichromic mirror, 510 nm; and barrier filter, 520 nm). H_2O_2 accumulation was detected by staining with 3,3'-diaminobenzidine (DAB; Amresco, Solon, OH, USA) as previously described (Wang *et al.*, 2007) and then viewed by differential interference contrast optics. Only the site where an appressorium had formed over a stoma was considered to be successfully penetrated. A minimum of 50 infection sites were examined on each of five randomly selected leaf segments for every treatment. The H_2O_2 accumulation, necrotic areas, hyphal length, and haustoria number were observed with a BX-53 microscope (Olympus) and calculated using DP-BSW software.

Statistical analysis

Microsoft Excel was used to calculate mean values and standard errors. To determine the significant differences between controls and treatments or between time-course points, the SPSS 16.0 statistical software was used to perform Student *t*-tests.

Accession numbers

The nucleotide sequences used in this study have the following GenBank accession numbers: *TaCBL1.1* (KU736847.1), *TaCBL2* (KU736848.1), *TaCBL3* (KU736849.1), *TaCBL4* (KU736850.1), *TaCBL6* (KU736851.1), *TaCBL9* (KU736852.1), *TaCIPK5* (KU736854.1), *TaEF-1a* (Q03033), *TaPR1* (AF384143), *TaPR2* (DQ090946), *TaSOD* (CB307850), *TaCAT* (X94352), and *TaNOX* (AY561153.1).

Results

Genome-wide identification and sequence analysis of wheat CBL *genes*

As the wheat genome database was updated recently, we identified the CBL sequences in *T. aestivum* cv. Chinese Spring again by HMM and BLAST searches. CBL protein sequences from Arabidopsis and rice were used as queries *in silico*. A total of 22 putative *CBLs* were identified in the wheat genome (seven, six, and nine loci in sub-genomes A, B, and D, respectively) and designated as *TaCBL1.1-1A* to *TaCBL9-3D*, following the designation used for rice through a comparison in InParanoid7 (http://inparanoid.sbc.su.se/cgi-bin/index.cgi) (Supplementary Table S1). In addition to *TaCBL1.1*, another candidate *CBL* gene showed high homology to *CBL1* from rice, and was thus designated as *TaCBL1.2*. In addition, a new *CBL* gene, *TaCBL8*, was identified. To confirm the evolutionary relationship of all putative TaCBLs with CBLs from Arabidopsis and rice, a phylogenetic tree was constructed based on the full-length amino acid sequences (Supplementary Fig. S1). The results showed that CBLs from various plants clustered in three major groups: type I, type II, and type III. TaCBLs were distributed among all three clusters, with the largest group, type I, containing 12 TaCBLs, while type II and type III contained seven and three members, respectively. Proteins belonging to the type I group began with a lipid modification motif (i.e. MGCXXS/T), and CBLs in the type II group contained the consensus motif MSQCXDGXKHXCXSXXXCF, which also existed in the tonoplast-targeting sequences (TTSs) of AtCBL2 and AtCBL3. Like AtCBL10, TaCBL9 possessed an extended N-terminus, which formed a transmembrane helix in members of the type III group (Supplementary Fig. S2).

TaCBL4 *is rapidly induced following infection of wheat with* Pst

Using the *TaCBL* sequences that we identified from the wheat genome, seven *TaCBLs* (1.1, 1.2, 2, 3, 4, 6, 9) from the wheat cv Suwon 11 were cloned out. During the interaction between wheat and *Pst*, expression profiles of these seven *TaCBLs* were confirmed by qRT-PCR. The transcript levels of all of them, with the exception of *TaCBL1.2* and *TaCBL6*, showed significant changes ($P<0.05$ and fold-change >2) in mRNA accumulation during incompatible (*Pst* race CYR23) and compatible (*Pst* race CYR31) interactions (Supplementary Fig. S3). Compared to the control, transcript levels of *TaCBL1.1* and *TaCBL2* were significantly induced at 6 hpi and reached a peak level of 2.5-fold higher during the incompatible interaction, whereas in the compatible interaction, these genes did not show significant changes at any time point (Supplementary Fig. S3A, C). The transcript levels of both *TaCBL3* and *TaCBL9* were down-regulated significantly by 24 hpi in the compatible interaction, but did not show significant changes in the incompatible interaction at any time point (Supplementary Fig. S3D, F). Among the *TaCBLs* evaluated, the level of *TaCBL4* was up-regulated significantly during interactions with CYR23 and CYR31 (Fig. 1). In the incompatible interaction, the transcript levels increased to a peak at 24 hpi, with a 3.5-fold increase over the control level. During the compatible interaction, *TaCBL4* was induced as early as 6 hpi and reached a peak level of expression that was a 3.8-fold increase compared to that in control-inoculated plants (Fig. 1). Based on these observations, *TaCBL4* was selected for further analysis during the response of wheat to *Pst* infection.

The deduced amino acid sequence and structural features of TaCBL4

TaCBL4 encodes a putative protein composed of 218 amino acid residues with a molecular weight of 24.8 kDa and an isoelectric point (pI) of 4.79 (Supplementary Table S1). The results of BlastN analysis indicated that the wheat genome contains three copies of *TaCBL4*, located on the long arms

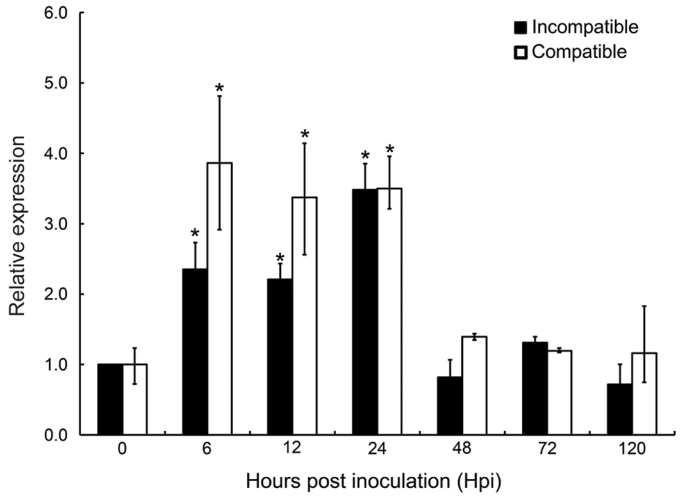

Fig. 1. *TaCBL4* is up-regulated during the interaction between wheat and *Pst*. Wheat leaves inoculated with *Pst* isolates CYR23 (incompatible interaction) and CYR31 (compatible interaction) were sampled and the relative transcript levels of *TaCBL4* were calculated by the comparative threshold ($2^{-\Delta\Delta CT}$) method. Wheat *TaEF-1α* was used as the reference. Data are means (±SE) of three biological replicates. The transcript level of *TaCBL4* in the leaves at time 0 was standardized as 1. Significant differences determined using Student's *t*-test are indicated: *P<0.05.

of chromosomes 1A, 1B, and 1D (Supplementary Figs S1, S4). The ORFs of each copy on the respective chromosomes were designated as *TaCBL4-1A*, *TaCBL4-1B*, and *TaCBL4-1D*. Each copy of *TaCBL4* was different from that identified previously (Sun *et al.*, 2015) (Supplementary Fig. S4). The *TaCBL4* gene from wheat cv Suwon11 exhibited 89.69%, 96.35%, and 88.74% identities with *TaCBL4-1A*, *TaCBL4-1B*, and *TaCBL4-1D*, respectively (Supplementary Fig. S5A). TaCBL4 from Suwon 11 contained the same number of amino acid residues and only a few amino acid variations relative to TaCBL4-1B, whereas TaCBL4-1A and TaCBL4-1D contained two and six amino acid deletions, respectively (Supplementary Fig. S5B). A multi-sequence alignment with all CBL proteins in Arabidopsis, rice, and wheat revealed that TaCBL4 contained four conserved EF-hand motifs (Supplementary Fig. S2).

Knockdown of TaCBL4 *reduces wheat resistance to* Pst

To characterize in more detail the role of *TaCBL4* during wheat responses to *Pst*, BSMV-VIGS, which has been applied to analyse gene function in wheat and barley, was used (Scofield *et al.*, 2005). Two *TaCBL4*-specific fragments were created for silencing (Supplementary Fig. S5A). At 10 dpi, all of the BSMV-inoculated plants displayed mild chlorotic mosaic symptoms, but had no obvious defects in further leaf growth. The plants inoculated with BSMV:TaPDS-as began to show photobleaching (Fig. 2A), indicating the initiation of BSMV-induced gene silencing compared with BSMV:γ-infected controls. The results of qRT-PCR to confirm the silencing efficiency indicated that the accumulation of *TaCBL4* transcripts was significantly reduced in *TaCBL4*-knockdown plants, with a reduction as high as 80% during the incompatible and compatible interactions (Fig. 2B). However, because of the high identity and similarity among the three copies on subgenomes A, B, and D, the expression level of each copy could not be determined (Supplementary Fig. S5A). Sequence alignment among all TaCBL members in wheat was performed to confirm the specificity of the fragments. As shown in Supplementary Fig. S6A, all TaCBLs lacked the consecutive 21- to 24-nucleotide sequences. Moreover, the expression of other *TaCBLs* was not suppressed in VIGS plants (Supplementary Fig. S6B), which confirmed the specificity of the fragments used in the VIGS assays (Supplementary Fig. S5A). At 10 dpi following *Pst* inoculation of the fourth leaf of wheat plants that had been pre-infected with BSMV:γ, BSMV:TaCBL4-1as, and BSMV:TaCBL4-2as, typical hypersensitive response (HR) symptoms appeared on all leaves after inoculation with CYR23 (Fig. 2C). At 15 dpi, a few fungal uredia surrounding the necrotic areas were observed on leaves previously infected with BSMV:TaCBL4-1as and BSMV:TaCBL4-2as (Fig. 2C). By contrast, normal disease development was exhibited on wheat leaves of *TaCBL4*-knockdown plants inoculated with the compatible strain, CYR31 (Fig. 2C).

To determine why leaves displayed reduced resistance to *Pst* when *TaCBL4* expression was reduced, we examined the fourth leaves microscopically to analyse the infection by CYR23 and CYR31 (Fig. 3, Supplementary Fig. S7). The necrotic area and H_2O_2 accumulation per infection site were significantly lower than those observed on BSMV-γ-infected leaves at 48 hpi and 120 hpi (P<0.05) in the incompatible interaction between wheat and *Pst* (Fig. 3A, C). Similarly, during the compatible interaction, at 48 hpi and 120 hpi we observed a decrease in the necrotic area and in H_2O_2 accumulation at the infection site compared to control plants (Supplementary Fig. S7A, B). To confirm the host response in *TaCBL4*-knockdown plants after *Pst* infection, the transcript levels of two pathogenesis-related (PR) protein genes and two ROS-scavenging genes were measured. During the compatible interaction between *TaCBL4*-knockdown plants and *Pst* (Supplementary Fig. S7C, D), knocking down *TaCBL4* resulted in a significant decrease in the transcript levels of *TaPR1* and *TaPR2*, as low as 80% at 24–120 hpi. *TaCAT* and *TaSOD*, the primary ROS-scavenging genes, were significantly increased in *TaCBL4*-knockdown plants challenged by CYR31 (Supplementary Fig. S7E, F).

In addition to analysing the host response, we also examined the number of haustoria, hyphal length, and infection area of *Pst* in *TaCBL4*-knockdown plants. After inoculation of the *Pst* avirulent race CYR23, hyphal length was not different between the two *TaCBL4*-knockdown and BSMV:γ-infected plants at 48 hpi (Fig. 4A, B). In contrast, hyphal length in infected leaves of both the BSMV:TaCBL4 plants was significantly higher than that in leaves of plants infected with BSMV:γ at 48 hpi in the compatible interaction (Supplementary Fig. S8A). The number of haustoria was significantly increased in both incompatible and compatible interactions at 48 hpi (Fig. 4A, C, Supplementary Fig. S8B). In addition, the infection area was significantly increased in *TaCBL4*-knockdown plants during incompatible and compatible interactions compared to the control (Fig. 4A, D; Supplementary Fig. S8C). Analysis showed that the biomass of *Pst* in *TaCBL4*-silenced plants was significantly increased at 5 dpi (Supplementary Fig. S9). Taken together, our results indicated that knockdown of expression of *TaCBL4* diminished plant defense against the stripe rust fungus.

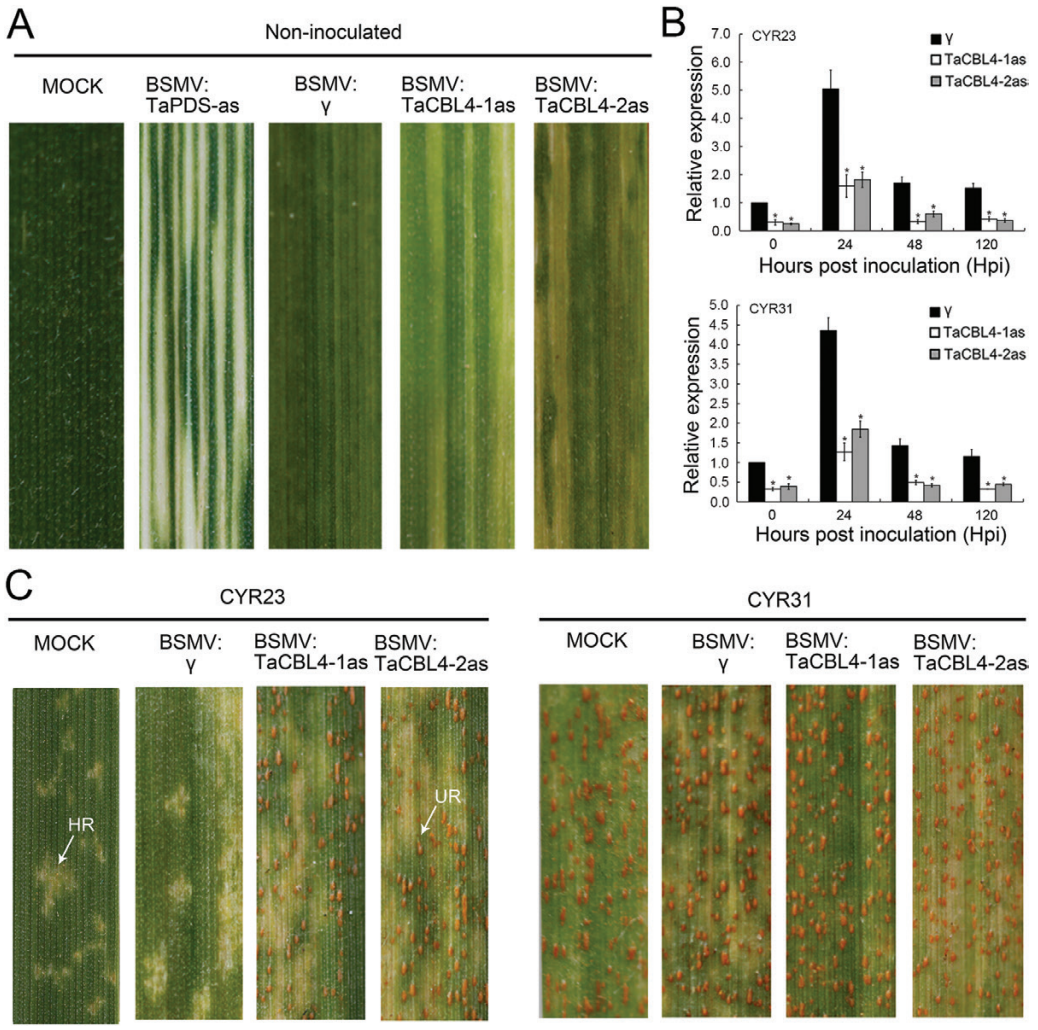

Fig. 2. *TaCBL4* is required for wheat resistance to *Pst*. (A) Mild chlorotic mosaic symptoms were observed on leaves inoculated with BSMV:γ, BSMV:TaPDS-as, BSMV:TaCBL4-1as, and BSMV:TaCBL4-2as at 10 d post-inoculation (dpi). Mock, wheat leaves treated with 1× FES buffer. (B) Relative transcript levels of *TaCBL4* in knockdown plants and control plants inoculated with the avirulent race CYR23 and the virulent race CYR31. RNA samples were isolated from the fourth leaves of plants first infected with BSMV:γ, BSMV:TaCBL4-1as, or BSMV:TaCBL4-2as and then inoculated with either CYR23 and CYR31. The data were normalized to the *TaEF-1α* gene. Wheat leaves infected only with BSMV:γ were used as controls. Significant differences from BSMV:γ as determined using Student's *t*-test are indicated: **P*<0.05. The relative level of *TaCBL4* in the control plants at time 0 was standardized as 1. (C) Images of the fourth leaves inoculated with urediospores of CYR23 or CYR31. Typical leaves at 15 dpi are shown. HR, hypersensitive response; UR, uredia. All results were obtained from three biological replicates. (This figure is available in colour at *JXB* online.)

TaCBL4 physically interacts with TaCIPK5 in vivo

To determine the interacting partner(s) of TaCBL4, a cDNA library constructed from *Pst*-infected leaves of *T. aestivum* cv. Suwon 11 was used for yeast-two hybrid (Y2H) screening. Using TaCBL4 as bait, a cDNA fragment of 2021 bp in length was identified with an ORF of 1395 bp, which showed high similarity to the CBL-interacting protein kinase-5 from *T. aestivum* cv. Chinese Spring. Amino acid sequences of putative CIPK5 orthologs from rice, barley, and maize were aligned (Supplementary Fig. S10). In addition, together with other CIPKs with assigned functions, a phylogenetic tree was constructed, which revealed that the CIPK gene obtained in this study lies within the same clade as HvCIPK5, BdCIPK5, ZmCIPK5, and OsCIPK5 (Fig. 5A). Based on this evidence, we designated the wheat CIPK as TaCIPK5. *In silico* sequence analysis indicated that the N- and C-terminals of TaCIPK5 contained a kinase catalytic domain and a regulatory domain, respectively. A putative trans-phosphorylatable threonine residue within the activation loop and a conserved ATP-binding lysine residue were found in the kinase catalytic domain, while the NAF/FISL region was in the regulatory domain (Supplementary Fig. S10). BlastN analyses of the wheat genome showed that there were two copies of *TaCIPK5* located on the short arms of chromosomes 3A and 3B (Supplementary Fig. S11). Sequence alignment showed that the two copies, designated as *TaCIPK5-A* and *TaCIPK5-B*, and *TaCIPK5* obtained in this study share 94% nucleotide identity (Supplementary Fig. S11). In addition, two copies of *TaCIPK5* were the same as those reported in a previous study (Sun *et al.*, 2015).

To confirm the interaction between TaCBL4 and TaCIPK5, the ORFs of *TaCBL4* and *TaCIPK5* were obtained and cloned, in-frame, into the Y2H vectors pGADT7 and pGBKT7, respectively. The interaction was monitored by yeast growth on the minimal selective medium lacking histidine, leucine,

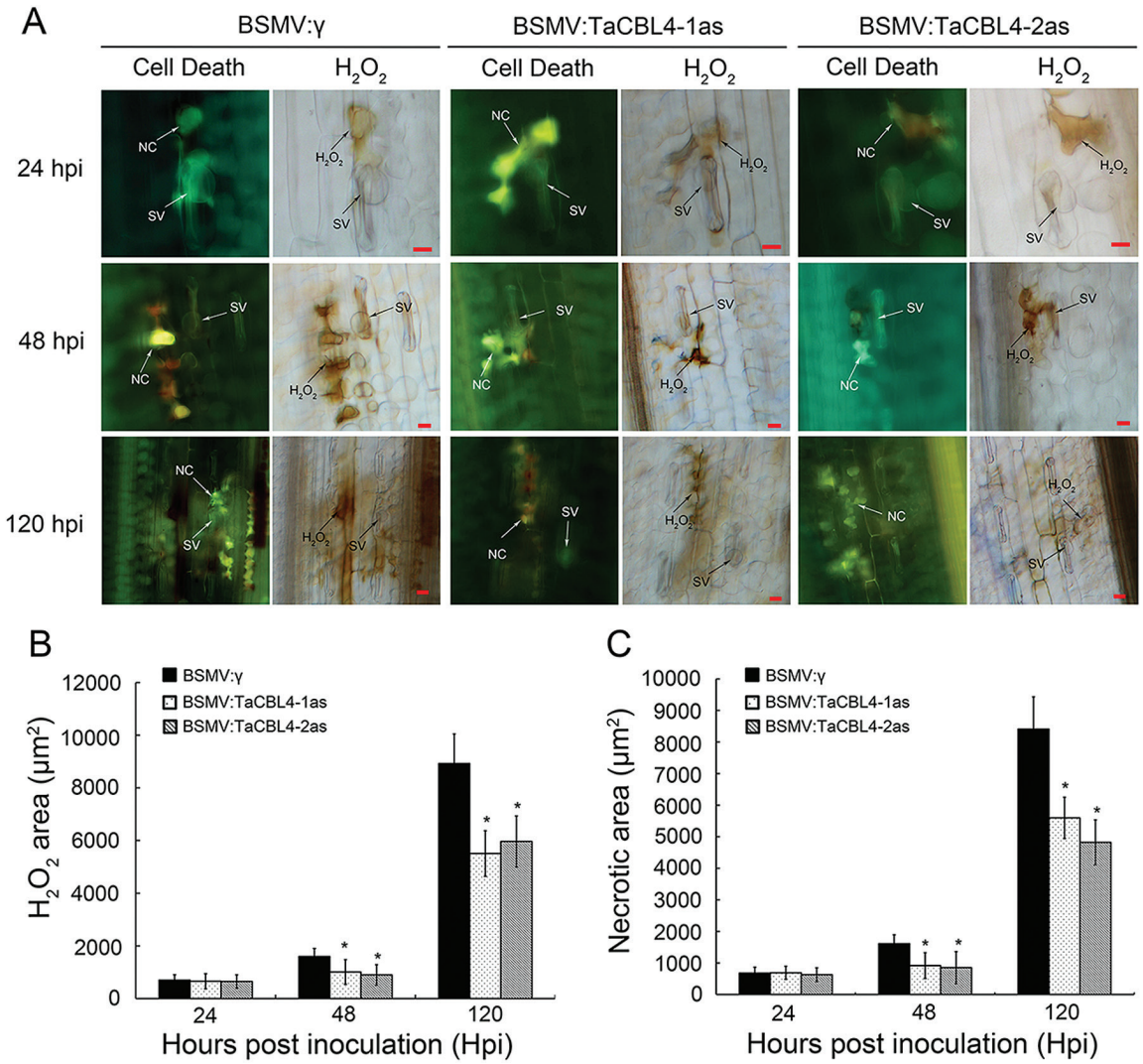

Fig. 3. Knock-down of *TaCBL4* reduces wheat defense responses to the avirulent *Pst* race CYR23. (A) Histological observations of wheat leaves treated with BSMV and infected with CYR23. Pre-infection of wheat leaves with BSMV:γ, BSMV:TaCBL4-1as, or BSMV:TaCBL4-2as was followed by inoculation with CYR23. H_2O_2 burst and necrosis were observed in these leaves at 24, 48, and 120 h post-inoculation (hpi). H_2O_2 accumulation at infection sites was detected by staining with 3,3-diaminobenzidine (DAB) and viewed under differential interference contrast optics. SV, substomatal vesicle; NC, necrotic cell. Scale bars are 20 μm. (B) The amount of H_2O_2 produced was measured by calculating the DAB-stained area at each infection site using the DP-BSW software. Data are means (±SE) of three independent assays. (C) The area of autofluorescence was measured to determine necrotic cell death. The results were obtained from 50 infection sites, and three biological replications were included. Significant differences compared to plants treated with BSMV:γ as determined using Student's *t*-test are indicated: *P<0.05. (This figure is available in colour at *JXB* online.)

tryptophan, and adenine but containing X-α-Gal (Fig. 5B). In addition, the interaction between TaCBL4 and TaCIPK5 was confirmed by Co-IP analysis with flag antibody. The NAF/FISL motif has been reported to interact with CBLs (Albrecht *et al.*, 2001). Mutant protein (TaCIPK5Δ) deficient in the FISL/NAF motif was generated (Supplementary Fig. S12). TaCIPK5Δ failed to interact with TaCBL4 in yeast and tobacco (Fig. 5B–D). The interaction between TaCIPK5Δ and TaCBL4 was further used as a negative control in the BiFC assay (Kudla and Bock, 2016), the results of which revealed yellow fluorescence signals distributed not only on the cell membrane but also within the cytoplasm when TaCIPK5 and TaCBL4 were co-expressed in the wheat cells (Fig. 5D). Western blot analysis confirmed that the expression of the mutant type TaCIPK5Δ fusion proteins was comparable to the expression of wild-type TaCIPK5. The expression of the TaCBL4 fusion protein and positive control were also detected by western blotting (Fig. 5E).

TaCIPK5 *positively regulates wheat resistance to* Pst

To determine whether *TaCIPK5* has a role in the defense of wheat against *Pst*, the expression patterns of *TaCIPK5* following biotic stress were investigated. Transcript abundance of *TaCIPK5* was induced as early as 6 hpi, with peak expression at 24 hpi in the incompatible interaction, whereas a significant change in *TaCIPK5* expression was not observed in the compatible interaction (Fig. 6A). To determine the genetic requirement, two *TaCIPK5* gene fragments were cloned and inserted into the VIGS-BSMV plasmid, and the resultant constructs, designated as BSMV:TaCIPK5-1as and BSMV:TaCIPK5-2as (Supplementary Fig. S11), were used to knockdown *TaCIPK5* by BSMV-VIGS.

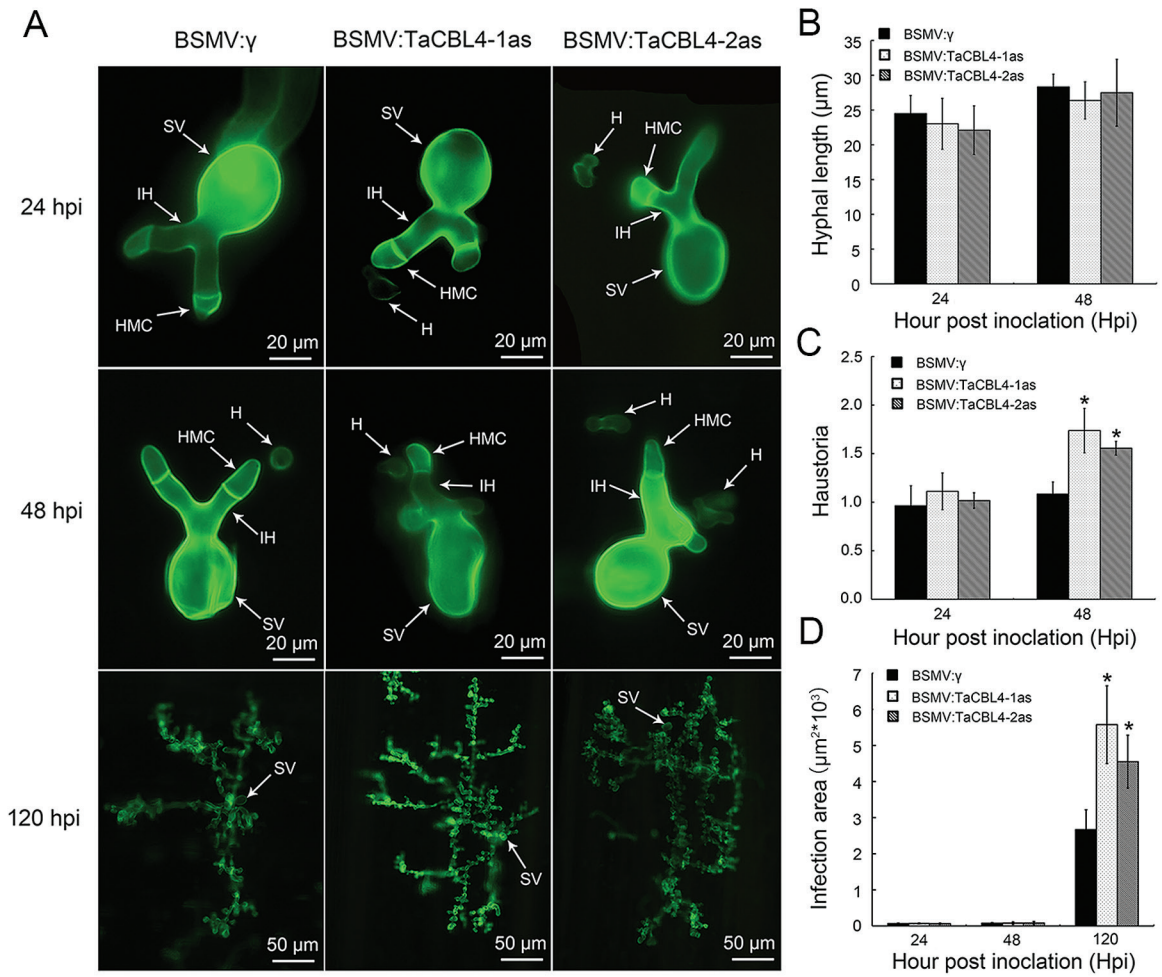

Fig. 4. Silencing *TaCBL4* in wheat induces growth of the *Pst* avirulent race, CYR23. (A) The fungal structures were stained with wheat germ agglutinin (WGA). The fungal growth of CYR23 in leaves inoculated with BSMV: γ, BSMV:TaCBL4-1as, or BSMV:TaCBL4-2as was observed under a fluorescence microscope at 24, 48, and 120 h post-inoculation (hpi). SV, substomatal vesicle; HMC, haustorial mother cell; IH, infection hypha. H, haustoria. (B) Hyphal length of CYR23, measured as the mean distance from the junction of the substomatal vesicle and the hypha to the tip of the hypha, was calculated using the DP-BSW software. (C) The average number of haustoria of CYR23 in each infection site. (D) Infection area of CYR23, measured as the mean of expanding hyphae, was calculated using the DP-BSW software. The results were obtained from 50 infection sites, and three biological replications were performed. Significant differences compared to plants treated with BSMV:γ as determined using Student's *t*-test are indicated: *P<0.05. (This figure is available in colour at *JXB* online.)

As shown in Fig. 6B, BSMV-inoculated plants displayed mild chlorotic mosaic symptoms at 10 dpi. The fourth leaf was inoculated with fresh urediospores of *Pst* CYR23 or CYR31, and the *TaCIPK5* transcript levels were reduced more than 45% at each time point (Fig. 6C). To confirm the specificity of the VIGS fragments used in this study, several *TaCIPK*s that fall in the same clade with TaCIPK5 (Sun *et al.*, 2015) were selected for sequence alignment. As shown in Supplementary Fig. S13A, no consecutive 21- to 24-nucleotide sequences were found among these *TaCIPK* genes. In addition, the expression of these *TaCIPK*s was not affected during the expression of resistance of TaCIPK5-knockdown plants to *Pst* (Supplementary Fig. S13B). By 15 dpi, large numbers of *Pst* uredia were formed around the necrotic spots on the leaves infected with BSMV:TaCIPK5-1as and BSMV:TaCIPK5-2as. In contrast, all leaves inoculated with CYR31 produced numerous uredia (Fig. 6D). Detailed histological changes of *TaCIPK5*-knockdown plants infected with CYR23 and CYR31 are shown in Fig. 7 and Supplementary Fig. S14. Compared to BSMV:γ-treated leaves, the areas of cell death and accumulation of H_2O_2 in *TaCIPK5*-knockdown plants were significantly lower in the incompatible interaction at 48 and 120 hpi (Fig. 7A, B) and in the compatible interaction at 120 hpi (Supplementary Fig. S14A, B). The number of haustoria and hyphal lengths in the *TaCIPK5*-knockdown plants infected with CYR23 (Fig. 7C, D) and CYR31 (Supplementary Fig. S14C, D) were significantly greater than those observed in the BSMV:γ-treated leaves at 48 hpi. The infection area was increased in both the *TaCIPK5*-knockdown plants inoculated with CYR23 or CYR31 (Fig. 7E, Supplementary Fig. S14E). The expression of *TaPR1* and *TaPR2* were both reduced significantly in *TaCIPK5*-knockdown plants when challenged with virulent race CYR31 (Supplementary Fig. S14F). *TaCAT* and *TaSOD* were significantly increased in the compatible interaction between *TaCIPK5*-knockdown plants and *Pst* (Supplementary Fig. S14G). In addition, analysis of biomass further confirmed that the *Pst* infection was significantly suppressed in *TaCIPK5*-knockdown plants at 5 dpi (Supplementary Fig. S15). Therefore, knocking down *TaCIPK5* reduces wheat resistance to *Pst*.

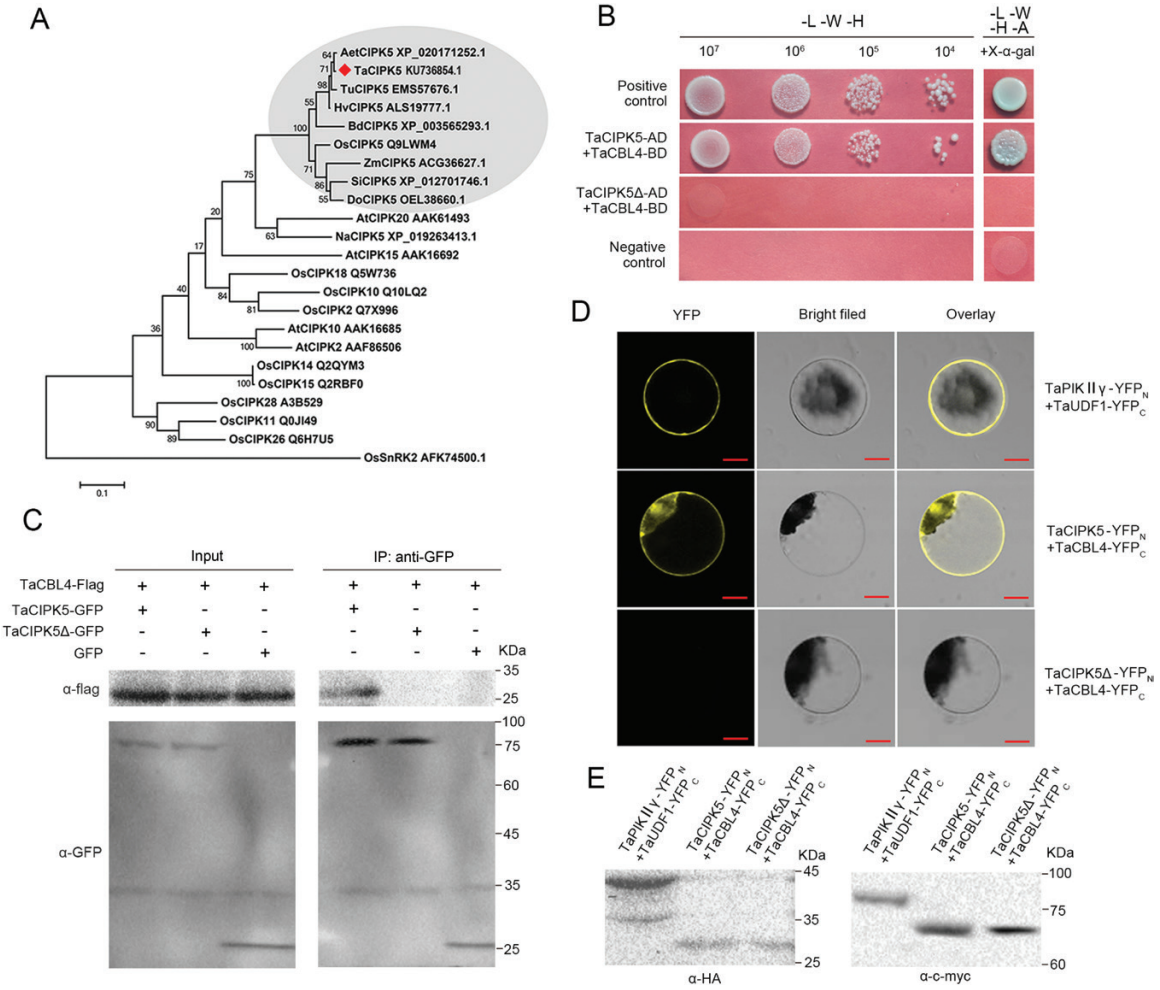

Fig. 5. TaCBL4 physically interacts with TaCIPK5. (A) Neighbor-Joining tree of CIPK5 protein sequences based on multiple alignments. The numbers at the branches indicate bootstrap values estimated based on 500 replications. Protein names and GenBank accession numbers are shown. Aet, *Aegilops tauschii*; Ta, *Triticum aestivum*; Tu, *Triticum urartu*; Hv, *Hordeum vulgare*; Bd, *Brachypodium distachyon*; Os, *Oryza sativa*; Zm, *Zea mays*; Si, *Setaria italic*; Do, *Dichanthelium oligosanthes*; At, *Arabidopsis thaliana*. OsSnRK2 was used as the outgroup. (B) Yeast two-hybrid analysis of interactions between TaCBL4 and TaCIPK5/TaCIPK5Δ. Cells of yeast strain AH109 harboring the indicated plasmid combinations were grown on selective media (SD–LWH and SD–LWHA containing 20 μg ml^{-1} X-α-gal). The interaction between SV40 large T-antigen (T) and murine p53 (53) T-AD+53-BD was used as the positive control, and the interaction between SV40 large T-antigen (T) and human lamin C (Lam), T-AD+Lam-BD was used as the negative control. (C) Protein–protein interactions between TaCBL4-FLAG constructs and TaCIPK5-GFP or TaCIPK5Δ-GFP constructs co-expressed in *Nicotiana benthamiana* were analysed by co-immunoprecipitation with an anti-GFP antibody followed by immunoblotting with anti-FLAG antibodies. Anti-GFP immunoprecipitated proteins were isolated 48 h after inoculation. Protein molecular weights are indicated to the right of the immunoblots. (D) *In vivo* bimolecular fluorescence complementation assays of interactions between TaCBL4 and TaCIPK5 or TaCIPK5Δ co-expressed in wheat protoplasts. YFP_N-TaPI4KIIγ+TaUDF1-YFP_C was the positive control and YFP_N-TaCIPK5Δ+TaCBL4-YFP_C was the negative control. Scale bars are 5 μm. (E) Protein expression determined by immunodetection with anti-HA (α-HA) antibodies for YFP_C fusions and anti-c-myc (α-c-myc) for YFP_N fusions. Proteins were extracted from wheat protoplasts co-transfected with the constructs indicated in (D). The molecular weights of the fusion proteins were as follows: YFP_N-TaPI4KIIγ, 85 kDa; YFP_N-TaCIPK5Δ, 64 kDa; YFP_N-TaCIPK5, 67 kDa; YFP_C-TaUDF1, 42 kDa; YFP_C -TaCBL4, 32 kDa. (This figure is available in colour at *JXB* online.)

Co-silencing of TaCBL4 *and* TaCIPK5 *significantly enhances wheat susceptibility*

To confirm the relationship between TaCBL4 and TaCIPK5 in wheat resistance to *Pst*, BSMV:TaCBL4-1as and BSMV:TaCIPK5-1as recombinant vectors were mixed together and rub-inoculated onto Suwon11 seedlings. To compare the disease resistance phenotype between single-silencing TaCBL4 and TaCIPK5 plants and co-silencing TaCBL4/TaCIPK5 plants, BSMV:TaCBL4, BSMV:TaCIPK5, or BSMV:TaCBL4/TaCIPK5 were separately inoculated. As shown in Fig. 8A, all BSMV-inoculated plants displayed mild chlorotic mosaic symptoms. After inoculation with fresh urediospores of *Pst* race CYR23, the relative expression of *TaCBL4* and *TaCIPK5* was significantly reduced in co-silenced plants compared with that in BSMV:γ-inoculated plants, suggesting that both TaCBL4 and TaCIPK5 were silenced successfully (Fig. 8B). At 15 dpi, large numbers of *Pst* uredia were produced around the necrotic spots on the leaves infected with BSMV:TaCBL4, BSMV:TaCIPK5, or BSMV:TaCBL4/TaCIPK5 (Fig. 8C). Histological changes in TaCBL4/TaCIPK5-knockdown plants infected with CYR23 were examined, and the areas of cell death and H_2O_2 accumulation

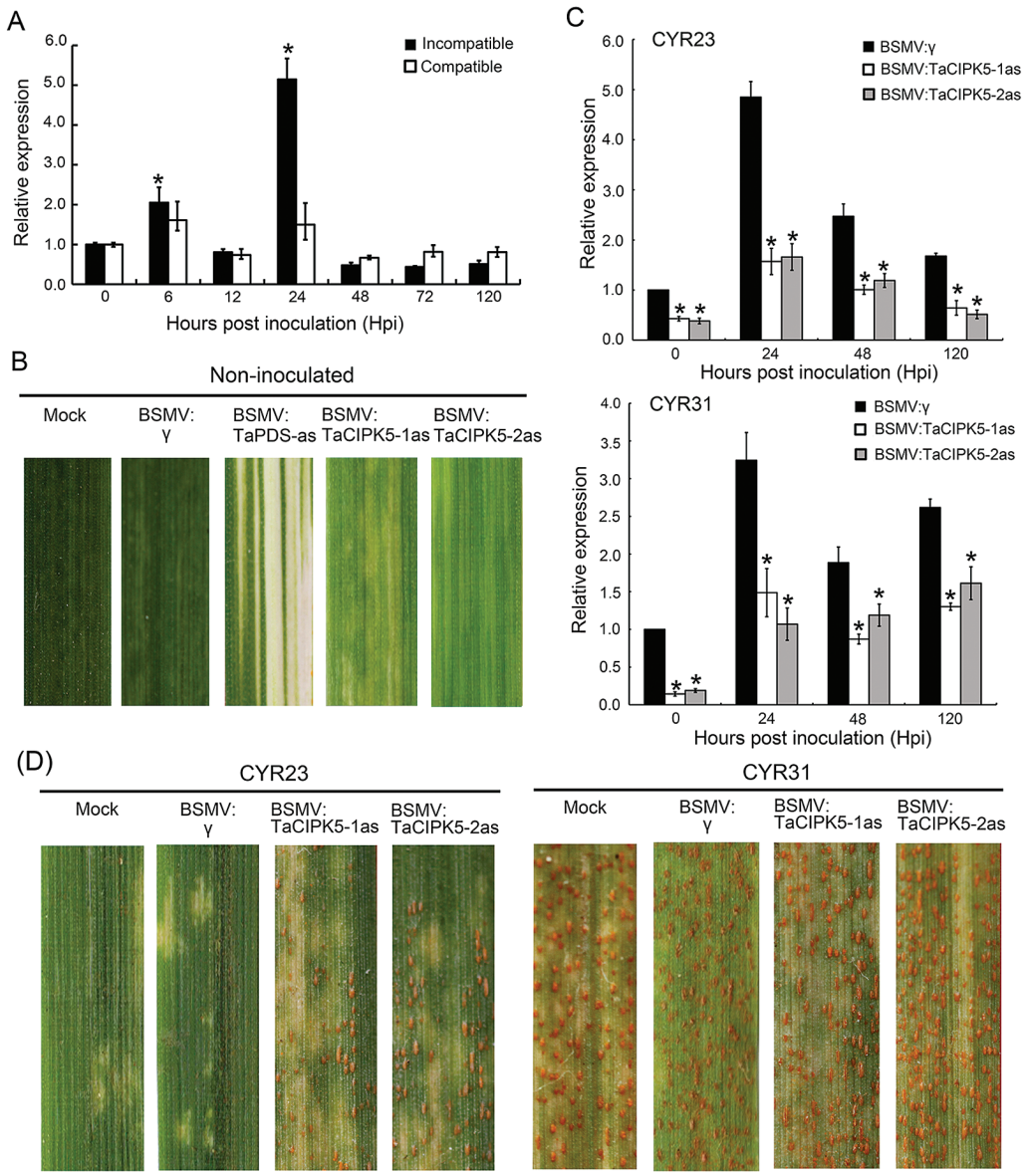

Fig. 6. *TaCIPK5* positively regulates wheat resistance to *Pst*. (A) Transcript profiles of *TaCIPK5* in response to infection in wheat leaves inoculated with *Pst* races CYR23 (incompatible interaction) and CYR31 (compatible interaction). Significant differences as determined using Student's *t*-test are indicated: **P*<0.05. (B) Mild chlorotic mosaic symptoms were observed on leaves inoculated with BSMV:γ, BSMV:TaPDS-as, BSMV:TaCIPK5-1as, and BSMV:TaCIPK5-2as at 10 d post-inoculation (dpi). Mock, leaves treated with 1× FES buffer. (C) Relative transcript levels of *TaCIPK5* in *TaCIPK5*-knockdown plants and control plants inoculated with CYR23 and CYR31. The data were normalized to the *TaEF-1a* gene. Plants inoculated with BSMV:γ were used as controls. The relative level of *TaCIPK5* in the control plants at time 0 was standardized as 1. Significant differences from BSMV:γ as determined using Student's *t*-test are indicated: **P*<0.05. (D) Images of fourth leaves inoculated with urediospores of CYR23 or CYR31. Typical leaves are shown at 15 dpi. (This figure is available in colour at *JXB* online.)

were significantly lower at 120 hpi than that observed in BSMV:γ-inoculated leaves (Supplementary Fig. S16A, B). The infection area was significantly increased in TaCBL4/TaCIPK5-knockdown plants (Supplementary Fig. S16C). The biomass of *Pst* in TaCBL4-, TaCIPK5-, and TaCBL4/TaCIPK5-knockdown plants was significantly increased compared to that in control plants at 15 dpi (Fig. 8D). Moreover, the biomass ratio (*Pst*/wheat) in co-silencing plants did not show a significant difference to that in all single-silencing plants (Fig. 8D). Compared to control plants, expression of all the *TaPR* genes was reduced significantly at 24–120 hpi in all single-knockdown plants and co-silencing plants when challenged with CYR23 (Fig. 8E), whereas *TaCAT* and *TaSOD* were significantly induced (Fig. 8F). These results showed that the expression patterns of *TaPR*s genes and ROS-related genes in co-silencing plants were consistent with those in single-silencing TaCBL4 and TaCIPK5 plants. In addition, the expression levels of *TaPR*s and ROS-related genes at each time point in co-silencing plants were not significantly different to those in single-silencing plants. Thus, co-silencing of *TaCBL4* and *TaCIPK5* significantly weakens wheat resistance against *Pst* infection and the disease-resistance phenotype in co-silencing plants is consistent with that in TaCBL4 and TaCIPK5 single-knockdown plants.

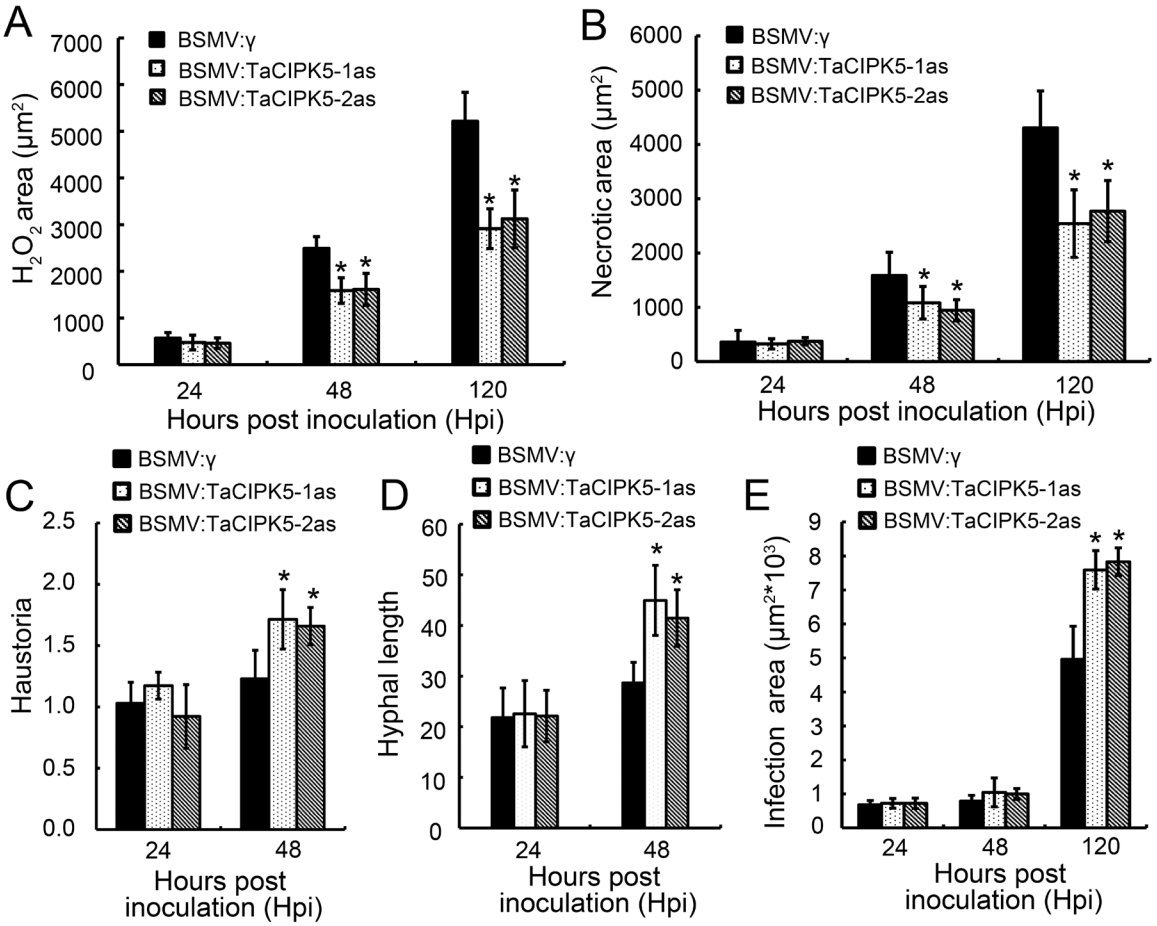

Fig. 7. Host responses and data from histological observations of fungal growth in *TaCIPK5*-knockdown plants challenged by avirulent CYR23. (A) The amount of H_2O_2 production was measured by calculating the DAB-stained area at each infection site using the DP-BSW software. Data are means (±SE) of three independent assays. (B) Necrotic cell death was quantified by measuring the area of autofluorescence. (C) The number of haustoria, (D) hyphal length, and (E) the infection area were determined using DP-BSW software. All results were obtained from 50 infection sites, and three biological replications were performed. Significant differences compared to BSMV:γ-inoculated plants as determined using Student's *t*-test are indicated: *P<0.05.

TaCIPK5 interacts with a wheat RBOH homolog protein

Several studies had been shown that the activation of RBOHs is regulated by CBL–CIPK complexes (Pandey *et al.*, 2014), and therefore we speculated that TaCIPK5 directly interacts with one of the RBOH proteins. A total of 11 RBOH-type genes were identified from *T. aestivum* in a genome-wide search and were designated as *TaRBOHa* to *TaRBOHi* based on their relationship to the respective genes in rice (Supplementary Figs S17A, S18). One of them was cloned in-frame into the pGBKT7 vector and the interaction between TaRBOH and TaCIPK5 was investigated using Y2H assays (Supplementary Fig. S17B). As shown in Supplementary Fig. S17C, TaCIPK5 strongly interacted with TaRBOHi. In addition, the relative expression of *TaRBOHi* was significantly reduced in TaCBL4-, TaCIPK5-, and TaCBL4/TaCIPK5-knockdown plants.

Discussion

Several CBL–CIPK interaction partners have been hypothesized to be involved in biotic and/or oxidative stress responses and developmental pathways, but evidence for this is sparse (Pandey *et al.*, 2014). In our present study, we demonstrated that most of the *TaCBL* genes are putatively involved with (or are at least responsive to) the interaction between wheat and *Pst*. Of these genes, we used a series of complementary cellular- and genetics-based assays to demonstrate that TaCBL4 and its interacting protein kinase, TaCIPK5, positively contribute to wheat resistance to *Pst*. Overall, the data that we present serve as a basis towards advancing our understanding of the role of the CBL–CIPK complex during fungal pathogen infection.

In a previous study, influx of Ca^{2+} from the intercellular space to the cytoplasm in wheat was found to be induced by *Pst* infection (Yin *et al.*, 2015). However, the downstream components of Ca^{2+}-regulated signaling in wheat resistance to *Pst* are still unknown. CBL proteins have been confirmed to interact with Ca^{2+} and transmit signals by activating the protein kinase of CIPKs (Pandey *et al.*, 2014). In our study, we observed rapid up- or down-regulation of *TaCBLs* during the response of wheat to *Pst*. Compared to the other *TaCBLs* that we isolated, *TaCBL4* showed the highest transcript level in both incompatible and compatible interactions, suggesting that it is a candidate gene required for wheat resistance-signaling in response to *Pst* infection. Previous studies have shown that the up-regulation of host genes during infection may indicate

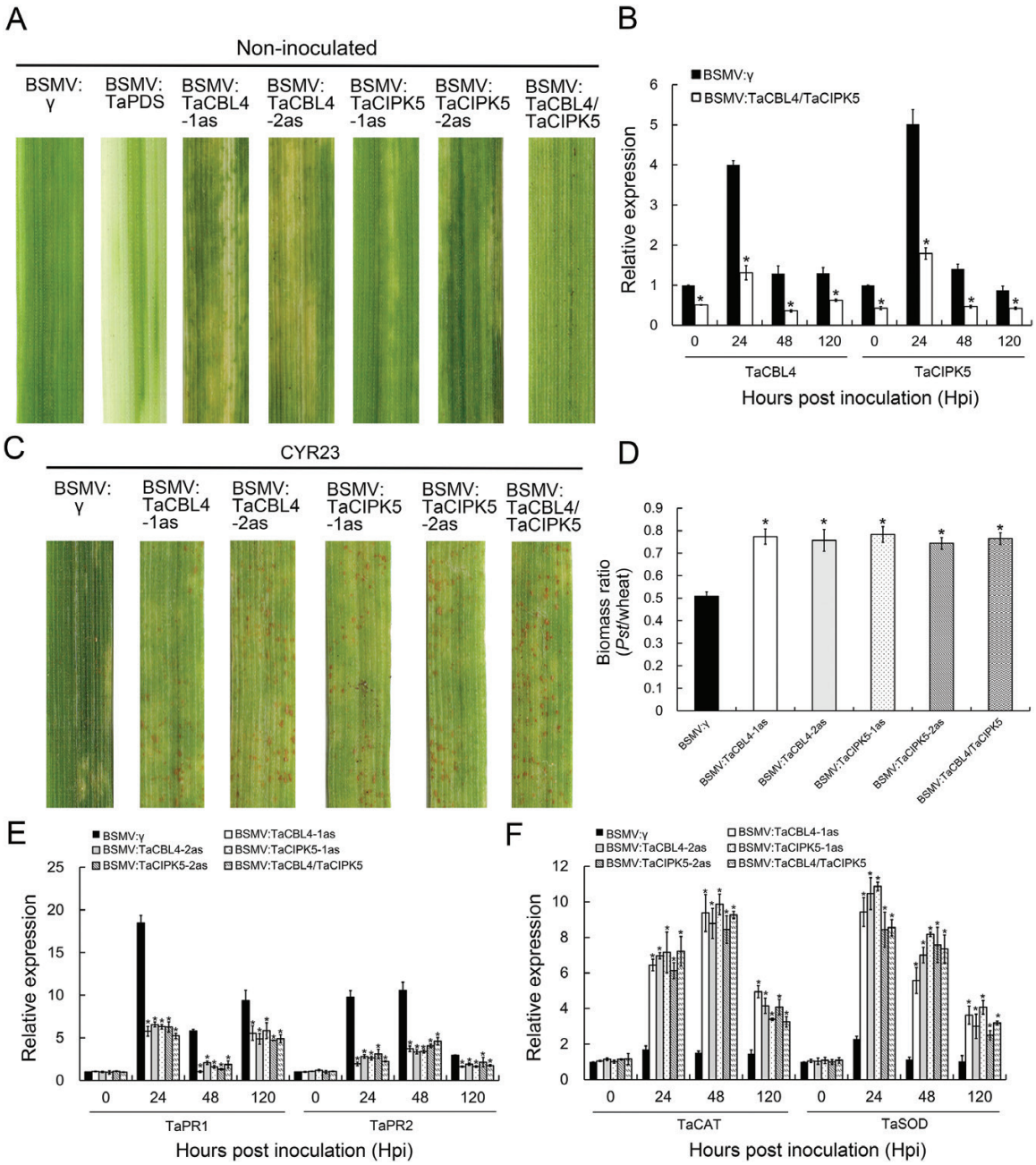

Fig. 8. Co-silencing of *TaCBL4* and *TaCIPK5* reduces wheat resistance to avirulent *Pst* race CYR23. (A) Mild chlorotic mosaic symptoms were observed on leaves inoculated with BSMV:γ, BSMV:TaPDS-as, BSMV:TaCBL4, BSMV:TaCIPK5, or BSMV:TaCBL4/TaCIPK5 at 10 d post-inoculation (dpi). (B) Relative transcript levels of *TaCIPK5* in control and *TaCBL4*/*TaCIPK5*-knockdown plants. The data were normalized to the *TaEF-1a* gene. Plants treated with BSMV:γ were used as the control. (C) Images of the fourth leaves inoculated with urediospores of CYR23 at 15 dpi. (D) Fungal and wheat biomass analysis in *TaCBL4*-, *TaCIPK5*-, and *TaCBL4*/*TaCIPK5*-silencing plants. The fungal and wheat biomass ratios were measured via total DNA content at 15 dpi by absolute quantification using the internal reference genes *PsEF* and *TaEF*, respectively. Relative transcript levels of (E) *TaPR1* and *TaPR2* and (F) *TaSOD* and *TaCAT* in *TaCBL4*-, *TaCIPK5*-, and *TaCBL4*/*TaCIPK5*-knockdown plants infected with CYR23. The relative transcript level of each gene in the control plants (treated with BSMV:γ) at time 0 was standardized as 1. Significant differences compared to BSMV:γ-inoculated plants as determined using Student's *t*-test are indicated: **P*<0.05. (This figure is available in colour at *JXB* online.)

the exploitation of cellular resources and/or the activation of defense responses (Wang *et al.*, 2010). Based on these results, we hypothesize that *TaCBL4* functions downstream of Ca^{2+} signals during the interaction between wheat and *Pst*. In addition, TaCIPK5, an interaction partner of TaCBL4, was identified by Y2H screening and further confirmed by BiFC and Co-IP. It has been shown that combinations of CBLs and CIPKs function as a signaling node in response to environmental stimuli (Thoday-Kennedy *et al.*, 2015). In a study of K^+ uptake, the CBL1/9–CIPK23 module was confirmed to regulate the potassium channel activity of AKT1 (Xu *et al.*, 2006). Another CBL–CIPK complex, CBL4–CIPK6, was shown to be required for translocation of AKT2 from the endoplasmic reticulum to the plasma membrane (Held *et al.*, 2011). However, the function of the CBL–CIPK complex in wheat remains unknown. In the present study, in addition to the interaction of TaCBL4

and TaCIPK5, the highest induction of *TaCBL4* and *TaCIPK5* occurred at the same time-point following CYR23 infection (Figs 2, 6A). Both TaCBL4 and TaCIPK5 played a positive role in wheat resistance, and the effect of TaCBL4 on ROS accumulation and PR gene expression was consistent with the effect of TaCIPK5. Moreover, the disease-resistance phenotype in plants with co-silencing of *TaCBL4* and *TaCIPK5* was consistent with that in plants with single-silencing. We confirmed that TaCIPK5 specifically functions with TaCBL4 to transmit Ca^{2+} signals to downstream immune signaling components during the interaction between wheat and *Pst*.

As a function of secondary signaling processes and the activation of anti-microbial/fungal responses, ROS has been well studied for its role in plant development and plant immunity (Lehmann *et al.*, 2015). In wheat, previous histological and cytological observations have demonstrated that bursts of ROS as early as 12 hpi are associated with the activation of defense signaling in incompatible interactions with *Pst* (Wang *et al.*, 2007). In our study, *TaCBL4* and *TaCIPK5* showed the highest induction during an incompatible interaction (Figs 2, 6A), with peak expression coinciding with the induction of ROS accumulation. This observation is in agreement with previous studies that demonstrated that the function of many CBL—CIPK complexes in abiotic and biotic stress signaling is associated with the burst of ROS (Pandey *et al.*, 2014). With respect to the function of the TaCBL4–TaCIPK5 complex, ROS accumulation was decreased compared to that in *TaCBL4*-, *TaCIPK5*-, and TaCBL4/TaCIPK5-knockdown plants infected with avirulent CYR23. Two major ROS-scavenging enzymes, superoxide dismutase (SOD) and catalase (CAT), could eliminate ROS accumulation (Mittler *et al.*, 2004). The accumulation of *TaSOD* and *TaCAT* transcripts in all types of silenced plants was induced by CYR23 (Fig. 8E, F). These results suggest that silencing the expression *TaCBL4* and *TaCIPK5* resulted in weakened ROS accumulation during wheat resistance. In addition, hypersensitive response (HR) is a common feature of wheat resistance, and is often induced and modulated by ROS. Hyphal length, number of haustoria, and infection area are representative of the extent of pathogen colonization in wheat under the stress imposed by HR at infection sites (Wang *et al.*, 2007). In all types of silenced plants infected with CYR23, the necrotic area of infection sites was significantly reduced compared with that in control plants, coinciding with decreased hyphal length and infection area. Our results suggest that the TaCBL4–TaCIPK5 complex positively contributes to wheat resistance against *Pst* in a ROS-dependent manner. In addition, we also confirmed that one of the wheat RBOHs, TaRBOHi, interacted with TaCIPK5 in a Y2H system. Similarly, the tomato CBL10–CIPK6 complex interacts with RBOHB at the plasma membrane to regulate ROS generation during effector-triggered immunity (de la Torre *et al.*, 2013). In addition, CIPK26 interacts with and phosphorylates RBOHF, and co-expression of either CBL1 or CBL9 with CIPK26 strongly enhances ROS production in HEK293T cells, demonstrating that the ROS production mediated by the CBL1/9–CIPK26 complex relies on the RBOH protein (Drerup *et al.*, 2013). Thus, we speculate that the ROS generation mediated by the TaCBL4-TaCIPK5 complex during wheat resistance to *Pst* depends on RBOH proteins. How RBOHs are regulated by the complex remains to be determined.

Salicylic acid (SA), a key signaling molecule of plant resistance against biotrophs, induces the expression of PR genes and results in systemic acquired resistance (SAR). Transcript levels of *TaPR1* and *TaPR2*, marker genes of the SA pathway (Van Loon, 1997), were significantly reduced in *TaCBL4*- and *TaCIPK5*-knockdown plants (Fig. 8E). Several studies have indicated that different Ca^{2+} sensors can modulate the elevation in SA that occurs late in immune responses (Tena *et al.*, 2011). In Arabidopsis, SA accumulation and PR gene expression are induced by CPK1 (Coca and San Segundo, 2010), while the CAM-binding transcription activator CAMTA3 (also called AtSR1) regulates SA-mediated plant immunity (Du *et al.*, 2009). Following treatment of rice cells with the fungal MAMP TvX/EIX, OsCIPK1-4/15 functions to promote PR gene expression, phytoalexin biosynthesis, and cell death, probably through the OsCBL4 Ca^{2+} sensor (Kurusu *et al.*, 2010). Thus, we infer that SA-mediated plant immunity in wheat is modulated by an activated TaCBL4–TaCIPK5 complex. Further investigation of this important signaling node will shed light on the activation of immunity following *Pst* infection of wheat.

In summary, we have demonstrated that the TaCBL4–TaCIPK5 complex positively contributes to wheat resistance to *Pst*. In addition, our results suggested that ROS generation is regulated by this complex through RBOH proteins, which activate the downstream signals during wheat resistance. Recent reports have shown that CIPK14/15 regulates defense gene expression and phytoalexin production in rice (Kurusu *et al.*, 2010). Furthermore, in tomato, ROS production is regulated by CBL10/CIPK6 (de la Torre *et al.*, 2013). Taken together, our study supports a role for CBL/CIPK in contributing to plant defense signaling and activation of immunity. We consider that knowledge of the regulatory mechanism of the TaCBL4–TaCIPK5 complex in ROS signaling will provide valuable insights into the molecular mechanism of plant immunity.

Supplementary data

Supplementary data are available at *JXB* online.

Fig. S1. Phylogenetic relationship of CBLs from wheat, Arabidopsis, and rice.

Fig. S2. Multiple alignment of CBL proteins from wheat, Arabidopsis and rice.

Fig. S3. Expression analysis of *TaCBLs* in response to *Pst*.

Fig. S4. Sequence alignment of *TaCBL4* identified in this study and in a previous study.

Fig. S5. Multiple sequence alignment of the coding sequences for the three copies of *TaCBL4*.

Fig. S6. Specificity analysis of VIGS fragments among all *TaCBL* members.

Fig. S7. Host responses in *TaCBL4*-knockdown plants challenged by virulent race CYR31.

Fig. S8. Data from histological observations of fungal growth in *TaCBL4*-knockdown plants challenged by the virulent race CYR31.

Fig. S9. Fungal and wheat biomass analysis in *TaCBL4*-knockdown plants.

Fig. S10. Multiple sequence alignment of TaCIPK5 with CIPK5 from other species.

Fig. S11. Multi-alignment of the cDNA sequence of the two copies of *TaCIPK5*.

Fig. S12. Schematic diagrams of TaCIPK5 mutants (TaCIPK5Δ).

Fig. S13. Specificity analysis of VIGS fragments among several *TaCIPK* members.

Fig. S14. Host responses and data from histological observations of fungal growth in *TaCIPK5*-knockdown plants challenged by the virulent race CYR31.

Fig. S15. Fungal and wheat biomass analysis in *TaCIPK5*-knockdown plants.

Fig. S16. Data from histological observations in *TaCBL4*/*TaCIPK5*-silencing plants challenged by the virulent race CYR31.

Fig. S17. TaCIPK5 interaction with TaRBOHi demonstrated in Y2H assays.

Fig. S18 CDS sequences of all identified *TaRBOH*s.

Table S1. Multiple alignments of CBL proteins from wheat, Arabidopsis, and rice, and motif analysis.

Table S2. Primers used in this study.

Acknowledgements

We thank Professor Larry Dunkle from the USDA-Agricultural Research Service at Purdue University, USA for critical reading of the manuscript. We also thank Professor Brad Day (Department of Plant, Soil and Microbial Sciences at Michigan State University, USA) for his efforts on improving the manuscript. This study was financially supported by the National Basic Research Program of China (No. 2013CB127700) and the National Natural Science Foundation of China (No. 31371889 and 31171795).

References

Abramovitch RB, Martin GB. 2005. AvrPtoB: a bacterial type III effector that both elicits and suppresses programmed cell death associated with plant immunity. FEMS Microbiology Letters **245,** 1–8.

Albrecht V, Ritz O, Linder S, Harter K, Kudla J. 2001. The NAF domain defines a novel protein–protein interaction module conserved in Ca^{2+}-regulated kinases. The EMBO Journal **20,** 1051–1063.

Campanella JJ, Bitincka L, Smalley J. 2003. Matgat: an application that generates similarity/identity matrices using protein or dna sequences. BMC Bioinformatics **4,** 29–29.

Cao Z, Jing J, Wang M, Shang H, Li Z. 2002. Relation analysis of stripe rust resistance gene in wheat important cultivar suwon 11, suwon 92 and hybrid 46. Acta Botanica Boreali-Occidentalia Sinica **23,** 64–68.

Clavijo BJ, Venturini L, Schudoma C, *et al*. 2017. An improved assembly and annotation of the allohexaploid wheat genome identifies complete families of agronomic genes and provides genomic evidence for chromosomal translocations. Genome Research **27,** 885–896.

Coca M, San Segundo B. 2010. AtCPK1 calcium-dependent protein kinase mediates pathogen resistance in Arabidopsis. The Plant Journal **63,** 526–540.

de la Torre F, Gutiérrez-Beltrán E, Pareja-Jaime Y, Chakravarthy S, Martin GB, del Pozo O. 2013. The tomato calcium sensor Cbl10 and its interacting protein kinase Cipk6 define a signaling pathway in plant immunity. Plant Cell **25,** 2748–2764.

Deng X, Hu W, Wei S, *et al*. 2013. *TaCIPK29*, a CBL-interacting protein kinase gene from wheat, confers salt stress tolerance in transgenic tobacco. PLoS ONE **8,** e69881.

Drerup MM, Schlücking K, Hashimoto K, Manishankar P, Steinhorst L, Kuchitsu K, Kudla J. 2013. The Calcineurin B-like calcium sensors CBL1 and CBL9 together with their interacting protein kinase CIPK26 regulate the *Arabidopsis* NADPH oxidase RBOHF. Molecular Plant **6,** 559–569.

Du L, Ali GS, Simons KA, Hou J, Yang T, Reddy AS, Poovaiah BW. 2009. Ca^{2+}/calmodulin regulates salicylic-acid-mediated plant immunity. Nature **457,** 1154–1158.

Du Y, Mpina MH, Birch PR, Bouwmeester K, Govers F. 2015. *Phytophthora infestans* RXLR effector AVR1 interacts with exocyst component Sec5 to manipulate plant immunity. Plant Physiology **169,** 1975–1990.

Duan Y, Guo J, Shi X, Guan X, Liu F, Bai P, Huang L, Kang Z. 2013. Wheat hypersensitive-induced reaction genes *TaHIR1* and *TaHIR3* are involved in response to stripe rust fungus infection and abiotic stresses. Plant Cell Reports **32,** 273–283.

Finn RD, Clements J, Eddy SR. 2011. HMMER web server: interactive sequence similarity searching. Nucleic Acids Research **39,** W29–W37.

Gupta DK, Palma JM, Corpas FJ. eds. 2015. Reactive oxygen species and oxidative damage in plants under stress. Heidelberg: Springer.

Hashimoto K, Eckert C, Anschütz U, Scholz M, Held K, Waadt R, Reyer A, Hippler M, Becker D, Kudla J. 2012. Phosphorylation of calcineurin B-like (CBL) calcium sensor proteins by their CBL-interacting protein kinases (CIPKs) is required for full activity of CBL-CIPK complexes toward their target proteins. The Journal of Biological Chemistry **287,** 7956–7968.

Hein I, Barciszewska-Pacak M, Hrubikova K, Williamson S, Dinesen M, Soenderby IE, Sundar S, Jarmolowski A, Shirasu K, Lacomme C. 2005. Virus-induced gene silencing-based functional characterization of genes associated with powdery mildew resistance in barley. Plant Physiology **138,** 2155–2164.

Held K, Pascaud F, Eckert C. *et al*. 2011. Calcium-dependent modulation and plasma membrane targeting of the AKT2 potassium channel by the CBL4/CIPK6 calcium sensor/protein kinase complex. Cell Research **21,** 1116–1130.

Ishitani M, Liu J, Halfter U, Kim CS, Shi W, Zhu JK. 2000. SOS3 function in plant salt tolerance requires N-myristoylation and calcium binding. The Plant Cell **12,** 1667–1678.

Kang Z, Huang L, Buchenauer H. 2002. Ultrastructural changes and localization of lignin and callose in compatible and incompatible interactions between wheat and *Puccinia striiformis*. Journal of Plant Diseases and Protection 25–37.

Kanwar P, Sanyal SK, Tokas I, Yadav AK, Pandey A, Kapoor S, Pandey GK. 2014. Comprehensive structural, interaction and expression analysis of CBL and CIPK complement during abiotic stresses and development in rice. Cell Calcium **56,** 81–95.

Kerppola TK. 2008. Bimolecular fluorescence complementation: visualization of molecular interactions in living cells. Methods in Cell Biology **85,** 431–470.

Kudla J, Bock R. 2016. Lighting the way to protein–protein interactions: recommendations on best practices for bimolecular fluorescence complementation analyses. The Plant Cell **28,** 1002–1008.

Kurusu T, Hamada J, Nokajima H, *et al*. 2010. Regulation of microbe-associated molecular pattern-induced hypersensitive cell death, phytoalexin production, and defense gene expression by calcineurin B-like protein-interacting protein kinases, OsCIPK14/15, in rice cultured cells. Plant Physiology **153,** 678–692.

Larkin MA, Blackshields G, Brown NP, *et al*. 2007. Clustal W and Clustal X version 2.0. Bioinformatics **23,** 2947–2948.

Lehmann S, Serrano M, L'Haridon F, Tjamos SE, Metraux JP. 2015. Reactive oxygen species and plant resistance to fungal pathogens. Phytochemistry **112,** 54–62.

Liu P, Xu ZS, Pan-Pan L, Hu D, Chen M, Li LC, Ma YZ. 2013. A wheat *PI4K* gene whose product possesses threonine autophophorylation activity confers tolerance to drought and salt in *Arabidopsis*. Journal of Experimental Botany **64,** 2915–2927.

Livak KJ, Schmittgen TD. 2001. Analysis of relative gene expression data using real-time quantitative PCR and the $2^{-\Delta\Delta C^T}$ method. Methods **25,** 402–408.

Luan S. 2009. The CBL-CIPK network in plant calcium signaling. Trends in Plant Science **14,** 37–42.

McNeal F, Konzak C, Smith E, Tate W, Russell T. 1971. A uniform system or recording and processing cereal research data. Agricultural Research Service, United States Department of Agriculture.

Mittler R, Vanderauwera S, Gollery M, Van Breusegem F. 2004. Reactive oxygen gene network of plants. Trends in Plant Science **9,** 490–498.

Mittler R, Vanderauwera S, Suzuki N, Miller G, Tognetti VB, Vandepoele K, Gollery M, Shulaev V, Van Breusegem F. 2011. ROS signaling: the new wave? Trends in Plant Science **16,** 300–309.

Pandey GK. 2008. Emergence of a novel calcium signaling pathway in plants: CBL-CIPK signaling network. Physiology and Molecular Biology of Plants **14,** 51–68.

Pandey GK, Kanwar P, Pandey A. 2014. Global comparative analysis of CBL-CIPK gene families in plants. Heidelberg: Springer.

Sanders D, Pelloux J, Brownlee C, Harper JF. 2002. Calcium at the crossroads of signaling. The Plant Cell **14,** S401–S417.

Sardar A, Nandi AK, Chattopadhyay D. 2017. CBL-interacting protein kinase 6 negatively regulates immune response to *Pseudomonas syringae* in *Arabidopsis*. Journal of Experimental Botany **68,** 3573–3584.

Scofield SR, Huang L, Brandt AS, Gill BS. 2005. Development of a virus-induced gene-silencing system for hexaploid wheat and its use in functional analysis of the *Lr21*-mediated leaf rust resistance pathway. Plant Physiology **138,** 2165–2173.

Steinhorst L, Kudla J. 2013. Calcium and reactive oxygen species rule the waves of signaling. Plant Physiology **163,** 471–485.

Sun T, Wang Y, Wang M, Li T, Zhou Y, Wang X, Wei S, He G, Yang G. 2015. Identification and comprehensive analyses of the *CBL* and *CIPK* gene families in wheat (*Triticum aestivum* L.). BMC Plant Biology **15,** 269.

Tamura K, Stecher G, Peterson D, Filipski A, Kumar S. 2013. MEGA6: Molecular evolutionary genetics analysis version 6.0. Molecular Biology and Evolution **30,** 2725–2729.

Tena G, Boudsocq M, Sheen J. 2011. Protein kinase signaling networks in plant innate immunity. Current Opinion in Plant Biology **14,** 519–529.

Thoday-Kennedy EL, Jacobs AK, Roy SJ. 2015. The role of the CBL-CIPK calcium signalling network in regulating ion transport in response to abiotic stress. Plant Growth Regulation **76,** 3–12.

Van Loon L. 1997. Induced resistance in plants and the role of pathogenesis-related proteins. European Journal of Plant Pathology **103,** 753–765.

Walter M, Chaban C, Schütze K, *et al*. 2004. Visualization of protein interactions in living plant cells using bimolecular fluorescence complementation. The Plant Journal **40,** 428–438.

Wan A, Zhao Z, Chen X, He Z, Jin S, Jia Q, Yao G, Yang J, Wang B, Li G. 2004. Wheat stripe rust epidemic and virulence of *Puccinia striiformis* f. sp. *tritici* in China in 2002. Plant Disease **88,** 896–904.

Wang CF, Huang LL, Buchenauer H, Han QM, Zhang HC, Kang ZS. 2007. Histochemical studies on the accumulation of reactive oxygen species (O^{2-} and H_2O_2) in the incompatible and compatible interaction of wheat–*Puccinia striiformis* f. sp. *tritici*. Physiological and Molecular Plant Pathology **71,** 230–239.

Wang X, Liu W, Chen X, *et al*. 2010. Differential gene expression in incompatible interaction between wheat and stripe rust fungus revealed by cDNA-AFLP and comparison to compatible interaction. BMC Plant Biology **10,** 9.

Wang X, Tang C, Zhang H, Xu JR, Liu B, Lv J, Han D, Huang L, Kang Z. 2011. *TaDAD2*, a negative regulator of programmed cell death, is important for the interaction between wheat and the stripe rust fungus. Molecular Plant-Microbe Interactions **24,** 79–90.

Wang Y, Sun T, Li T, Wang M, Yang G, He G. 2016. A CBL-interacting protein kinase TaCIPK2 confers drought tolerance in transgenic tobacco plants through regulating the stomatal movement. PLoS ONE **11**, e0167962.

Xiang Y, Huang Y, Xiong L. 2007. Characterization of stress-responsive *CIPK* genes in rice for stress tolerance improvement. Plant Physiology **144**, 1416–1428.

Xie C, Zhou X, Deng X, Guo Y. 2010. PKS5, a SNF1-related kinase, interacts with and phosphorylates NPR1, and modulates expression of *WRKY38* and *WRKY62*. Journal of Genetics and Genomics **37,** 359–369.

Xu J, Li H, Chen L, Wang Y, Liu L, He L, Wu W. 2006. A protein kinase, interacting with two calcineurin B-like proteins, regulates K^+ transporter AKT1 in Arabidopsis. Cell **125,** 1347–1360.

Xu W, Jia L, Shi W, Baluska F, Kronzucker HJ, Liang J, Zhang J. 2013. The tomato 14-3-3 protein TFT4 modulates H^+ efflux, basipetal auxin transport, and the PKS5-J3 pathway in the root growth response to alkaline stress. Plant Physiology **163,** 1817–1828.

Yang Y, Zhao J, Liu P, Xing H, Li C, Wei G, Kang Z. 2013. Glycerol-3-phosphate metabolism in wheat contributes to systemic acquired resistance against *Puccinia striiformis* f. sp. *tritici*. PLoS ONE **8,** e81756.

Yin S, Wang C, Jiao M, Li F, Han Q, Huang L, Zhang H, Kang Z. 2015. Subcellular localization of calcium in the incompatible and compatible interactions of wheat and *Puccinia striiformis* f. sp. *tritici*. Protoplasma **252,** 103–116.

Zurbriggen MD, Carrillo N, Hajirezaei MR. 2010. ROS signaling in the hypersensitive response: when, where and what for? Plant Signaling & Behavior **5,** 393–396.